Preprint Cambridge Centre for Computational Chemical Engineering ISSN 1473 – 4273

An Improved Methodology for Determining Threshold Sooting Indices from Smoke Point Lamps

Roger Watson [1], Christopher Ness [1], Neal Morgan [2], Markus Kraft [1]

Draft of December 20, 2011

[1] Department of Chemical Engineering and Biotechnology
University of Cambridge
New Museums Site
Pembroke Street
Cambridge, CB2 3RA
United Kingdom
E-mail: mk306@cam.ac.uk

[2] Shell Global Solutions (UK) (A division of Shell Research Ltd)
Shell Technology Centre
Thornton
Pool Lane
Ince, CH2 4NU
E-mail: N.Morgan@shell.com

Preprint No. 110

Keywords: c4e, preprint, template

Edited by
Computational Modelling Group
Department of Chemical Engineering and Biotechnology
University of Cambridge
New Museums Site
Pembroke Street
Cambridge CB2 3RA
United Kingdom

Fax: + 44 (0)1223 334796
E-Mail: c4e@cam.ac.uk
World Wide Web: http://como.cheng.cam.ac.uk/

Abstract

The ASTM D1322 smoke point test has been used for many years as a quick, convenient and easy way to characterize the sooting propensity of aviation fuels. Attempts to apply the same procedure to hydrocarbons in general have been less successful, since for highly sooting fuels the low smoke point makes it very difficult to obtain values with adequate reproducibility. This work describes an adapted version of the test which is usually much more reproducible than the ASTM method, particularly in the case of highly sooting fuels; typically halving the experimental error. The only additional equipment required is an analytical balance of 0.1 mg precision and a PC, together with some modifications to the ASTM D1322 burner which can be carried out in most engineering workshops. The alternative test is based on the fuel uptake rate, rather than the height of the flame, which makes it more susceptible to systematic errors from fuel vapour loss, however a means of identifying cases where this error is significant is proposed.

Contents

1 Introduction

Airborne particulate matter is known to adversely affect human health in many ways; causing harm to the lungs, heart, bloodstream, cardiovascular system and brain [14]. A significant source of this particulate matter is soot generated from internal combustion engines. In order to assess the environmental impact of a given fuel blend, there are two major requirements:

1. An objective measure of the overall sooting propensity of the fuel blend;
2. Information about the particles size distribution (PSD), as particles of diameter below 100 nm are significantly more harmful than larger particles, as well as remaining airborne for much longer [19].

Ultimately, a predictive model to describe both the sooting propensity and the PSD is required, and some progress has already been made towards this goal ([12], [15], [16], [21]), however experimental data are required to aid model development. This work will focus on the simpler problem of how to quantify sooting propensity based on robust and reproducible measurements.

A widely used metric for the sooting propensity of a fuel is the ASTM D1322 smoke point test; particularly in the case of aviation fuels. The test uses a standardized apparatus involving a wick-fed laminar diffusion flame to quantify sooting propensity in terms of the height of the flame for incipient production of visible soot. This height is known as the smoke point. According to the ASTM standard, the process of obtaining the smoke point requires that the flame be progressed through the following stages:

1. A long tip; smoke slightly visible; erratic and jumpy flame.
2. An elongated, pointed tip with the sides of the tip appearing concave upward as shown in **Figure** 1a (Flame A).
3. The pointed tip just disappears, leaving a very slightly blunted flames as shown in Figure 1a (Flame B). Jagged, erratic, luminous flames are sometimes observed near the true flame tip; these shall be disregarded.

The height of the flame at point B is recorded to the nearest 0.5 mm, and three separate measurements are taken.

Despite the efforts of the writers of ASTM D1322 to clearly define the smoke point, there is still a level of subjectivity in the measurement; which is reflected in the ± 3 mm reproducibility estimate quoted in the standard. This level of error is acceptable for low-to-medium sooting propensity fuels such as isooctane, but is a severe problem for fuels such as toluene which typically has a smoke point of around 6 mm. Reduction or elimination of the subjective elements of the test would therefore be a welcome development.

A characteristic of the smoke point which is used in some literature, e.g. Glassman and Yaccarino [6], is the presence of 'sooting wings'. These appear as a weakly luminescent

region near the top of the flame with clearly defined sides, but no clear upper boundary, as illustrated in **Figure** 1b. Unfortunately sooting wings are not usually observable for fuels with a high sooting propensity, and are therefore unsuitable as a universal criterion for the smoke point.

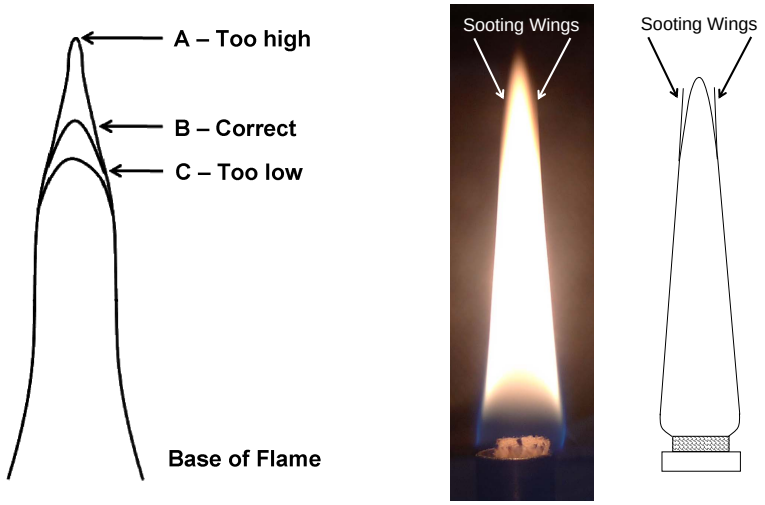

(a) *Determination of the Smoke Point according to ASTM D1322.*

(b) *Sooting wings for an iso-octane flame at its smoke point*

Figure 1: *Definition of the smoke point*

The **purpose of this paper** is to present the findings of an in-depth investigation into the smoke point test and explore how its accuracy, reproducibility and range of applicability can be enhanced. More specifically, the objectives are to:

- investigate the relationship between fuel uptake rate and flame height, as earlier literature [13] suggests that this may deviate from linear at the smoke point;
- use this information to develop a more precise and objective measure of sooting tendency, whilst retaining as much of the simplicity of the standard test as possible;
- investigate any further inherent weaknesses in the test.

2 Characterization of Sooting Propensity

2.1 Calculating the Threshold Sooting Index

In practice, many of the experimental setups described in the literature do not conform to the design specified in ASTM D1322. The main reasons for this are that:

- the ASTM lamp is difficult to use with additional diagnostics, such as lasers or particle sampling probes;
- the lamp is designed for aviation fuels and is unsuited to gaseous fuels, low-sooting fuels such as n-heptane or very strongly sooting fuels such as naphthalene.

The smoke point is known to be a function of the apparatus design [17], meaning that some form of common standard is needed for smoke point measurements to be meaningful. Minchin [11] suggested that any such standard could have a simple inverse proportional relationship with the smoke point (h), measured in mm, however Calcote and Manos [3] noted that this approach failed to account for the effect of stoichiometric ratio on flame height. In order to solve this problem Calcote and Manos [3] instead proposed a 'Threshold Sooting Index' (TSI), in which '0' = 'least sooting' and '100' = 'most sooting'. Assuming that the stoichiometric ratio was linearly related to the fuels' molecular weight (M_W), as well as allowing for some level of linear offset, this assumption lead to equation (1):

$$\text{TSI} = a_h \left(\frac{M_W}{h} \right) + b_h \tag{1}$$

where a_h and b_h are apparatus-dependent constants if the smoke point is used.

Some authors, such as Street and Thomas [20] and Blazowski [1] based their sooting propensity measurements on the 'critical equivalence ratio' (ϕ_e) at which soot was first produced in a premixed flame. For such experiments Calcote and Manos proposed that equation (2) be used to determine TSI:

$$\text{TSI} = a_e - b_e \phi_e \tag{2}$$

where a_e and b_e are apparatus-dependent constants if the equivalence ratio is used.

It was also advocated that TSI could be defined in terms of the volumetric flow rate of fuel, as is shown in equation (3). The basis for this relation was the theory of Burke and Schumann [2], which predicted a proportional relationship between fuel volumetric flow (V) rate and flame height.

$$\text{TSI} = a_V \left(\frac{M_W}{\dot{V}} \right) + b_V \tag{3}$$

where a_h and b_h are apparatus-dependent constants if the volumetric flow rate is used.

In order to use all of these methods, arbitrary TSI values must be assigned to two reference fuels (indicated by subscripts 1 and 2) which can then be burned in the apparatus of interest. It is then possible to determine the apparatus-dependent constants a and b by simultaneous solution. For the smoke point method this would yield equations (4) and (5):

$$a_h = \frac{\text{TSI}_1 - \text{TSI}_2}{\left(\frac{M_{W1}}{h_1} \right) - \left(\frac{M_{W2}}{h_2} \right)} \tag{4}$$

$$b_h = \frac{\text{TSI}_1 \left(\frac{M_{W2}}{h_2}\right) - \text{TSI}_2 \left(\frac{M_{W1}}{h_1}\right)}{\frac{M_{W2}}{h_2} - \frac{M_{W1}}{h_1}} \tag{5}$$

It is also possible to determine a and b more precisely by least-squares fitting of smoke point data plotted against literature TSI values [13], however this approach is best avoided as it inevitably adds a certain amount of circularity to the analysis and consequently reduces the scientific validity of the results.

2.2 Strengths and Weaknesses of the TSI Metric

The TSI is useful because it has been found (Gill and Olson [5]) to blend linearly with mole fraction, as described by equation (6):

$$\text{TSI}_{blend} = \sum x_f \text{TSI}_{Pure} \tag{6}$$

The TSI is also of interest because it has been shown to be a good predictor of the amount of soot produced by real engines [22]. In its current form, the methodology for determining TSI nevertheless has a number of shortcomings:

1. The correlations for TSI are empirical in nature and the coefficients a and b have no basis in theory other than the inclusion of the M_W term in some of its forms. Even if the metric works well as a predictive tool in selected cases, its fundamental basis is still not understood, meaning that results cannot be extrapolated with confidence.

2. It is currently difficult to assess the limitations of the TSI methodology, i.e. its transferability between different experimental setups, because of the high level of experimental error in much of the relevant data. For example McEnally and Pfefferle [9] state that the average 95% confidence limit is $\pm 15\%$ for TSIs obtained using the smoke point method, although this figure can be much higher for strongly sooting fuels.

3. There is no widely recognized standard list of TSI values, meaning that the author has to assign reasonable values to a reference fuel based on what has already been reported in the literature. For example, Calcote and Manos [3] suggest TSI $= 2$ for n-hexane and TSI $= 100$ for 1-methyl naphthalene, whereas Mensch et al. [10] suggest using methylcyclohexane with TSI $= 5$ as the lower bound. Although Olson et al. [13] suggest some TSI reference values for a wide range of fuels, the uncertainties in these values are still unacceptably high; a further reason why better experimental methods are needed.

2.3 Other Approaches

A proposal to improve the repeatability of sooting tendency measurements was recently made by McEnally and Pfefferle [9], who suggested the 'Yield Sooting Index' (YSI) as an

alternative to the TSI. In the YSI test, laser incandescense is used to measure the maximum soot volume fraction, $f_{v,max}$ in a coflow methane/air non-premixed flame in which the fuel is doped with 400 ppm of the test hydrocarbon. In the same way that smoke points are converted into apparatus independent TSIs, the $f_{v,max}$ values are converted into YSIs according to equation (7) in order to characterize sooting tendency:

$$YSI = Cf_{v,max} + D \tag{7}$$

where C and D are apparatus-dependent coefficients which must be experimentally derived based on the results for benzene (YSI = 30) and 1,2-dihydronaphthalene (YSI = 100). McEnally and Pfefferle [9] reported that the correlation coefficient between their YSI values and a set of 18 TSI values obtained by Olson et al. [13], was 0.84; a relatively high value given the large uncertainties in the TSIs, indicating that YSI and TSI may be interchangeable. Further to this, the quoted uncertainty of YSI values was 3%, provided that the correct amount of dopant is added to the flame; a significant improvement over that for the TSI. Following a further publication by McEnally and de Pfefferle [8], YSI data are now available for a wide range of fuels.

Another alternative standard, named the Micropyrolysis Index (MPI), was developed by Crossley et al. [4]. The main objective of this approach was to obtain a result that was independent of operating conditions such as temperature and oxygen supply. Pyrolysis of the test fuel was carried out at 850°C in a bed of R-Al_2O_3 beads. The amount of deposited carbon was then quantified using 'Temperature Programmed Oxidation' in order to quantify the sooting tendency of the fuel. The correlation between TSI and MPI was not as strong at that with YSI, although Crossley et al. [4] do not quote a figure and the data set they use is much more limited.

The main disadvantage of the YSI and MPI approaches, is that they require a greater level of investment than the smoke point method; both in terms of the cost of the equipment and in the technical knowledge and experience needed to use them.

2.4 Adapted Smoke Point Test

Earlier work by Olson et al. [13] suggested that the smoke point method could be modified by measuring the fuel uptake rate at the smoke point, rather than the smoke point itself; indeed this approach was used in earlier work by Schalla and McDonald [18]. Thus, the TSI would be given by equation (8):

$$\text{TSI} = a_m \left(\frac{M_W}{\dot{m}} \right) + b_m \tag{8}$$

The basis for this suggestion was an observation reported by Jezl [7] that when experimental measurements of flame height were plotted against fuel uptake rate, the smoke point occurred at a distortion in the resulting curve. There were thought to be two main advantages of using the fuel uptake rate as opposed to the flame height; firstly it could be measured more precisely and secondly the shape of the distortion was thought to be such that the fuel uptake rate would not be very sensitive to the flame height in the region

around the smoke point. Mensch et al. [10] claimed that the uncertainty of the method was $\pm$ 7%, although Olson et al. [13] imply that this was merely the readability of the uptake rate measurement, without accounting for other factors such as human error. Further verification is therefore required before it can be conclusively stated that the fuel uptake rate method is better than the smoke point method for determining TSI.

3 Experimental Methods

3.1 Relationship Between Flame Height and Fuel Uptake Rate

Olson et al. [13] included some plots of fuel uptake rate vs flame height in their work, in which a distortion could be observed around the smoke point. Unfortunately there were insufficient data to show the shape of the distortion, or even to show conclusively that it existed. An improved methodology and laboratory setup (**Figure** 2) were therefore developed in order to confirm the findings of Olson et al..

The height of the flame was automatically adjusted in small increments by using the linear displacement motor to change the wick exposure. For each flame height, the mass of the burner and its contents was logged for a minimum of 1 minute using LabX direct software and a Mettler-Toledo EL204-IC analytical balance of readability 0.1 mg. The gradient of the least-squares regression line was then used to determine the fuel uptake rate, after rejection of any data that clearly deviated from linear. Excellent linearity was nevertheless obtained in the majority of cases. Typical raw data obtained from this approach are shown in **Figure** 3, although individual data points are not distinguishable due to the high frequency of sampling.

The flame height itself was measured with the aid of a Logitech 9000 Webcam, which was used in 1280 $\times$ 720 mode at 20 frames per second. A calibration rod of length 100mm was inserted into the wick sheath and its length measured directly from the screen of the associated PC monitor. The number of pixels, N_P, per real-life millimeter was therefore given by equation (9):

$$\frac{N_P}{H_{real}} = \frac{720}{100}\frac{H_{rod}}{H_{vid}} \tag{9}$$

where H_{real}, H_{rod}, and H_{vid} were the heights (in mm) respectively of the real-life measurement, the calibration rod as it appeared on the screen, and the video frame as it appeared on the screen; as shown in **Figure** 4.

The camera was positioned such that the rod occupied most of the screen, so that a resolution of better than 0.2mm could be obtained. Footage was recorded over approximately the same duration as the mass measurements, then converted from .wav format to .avi format using 'Prism video convertor' software, so that it was possible to carry out image analysis using MATLAB. Images were converted to greyscale and cropped at the base of the flame, then converted to binary format by application of a light intensity threshold which was chosen to be high enough to eliminate reflections on the acrylic panel.

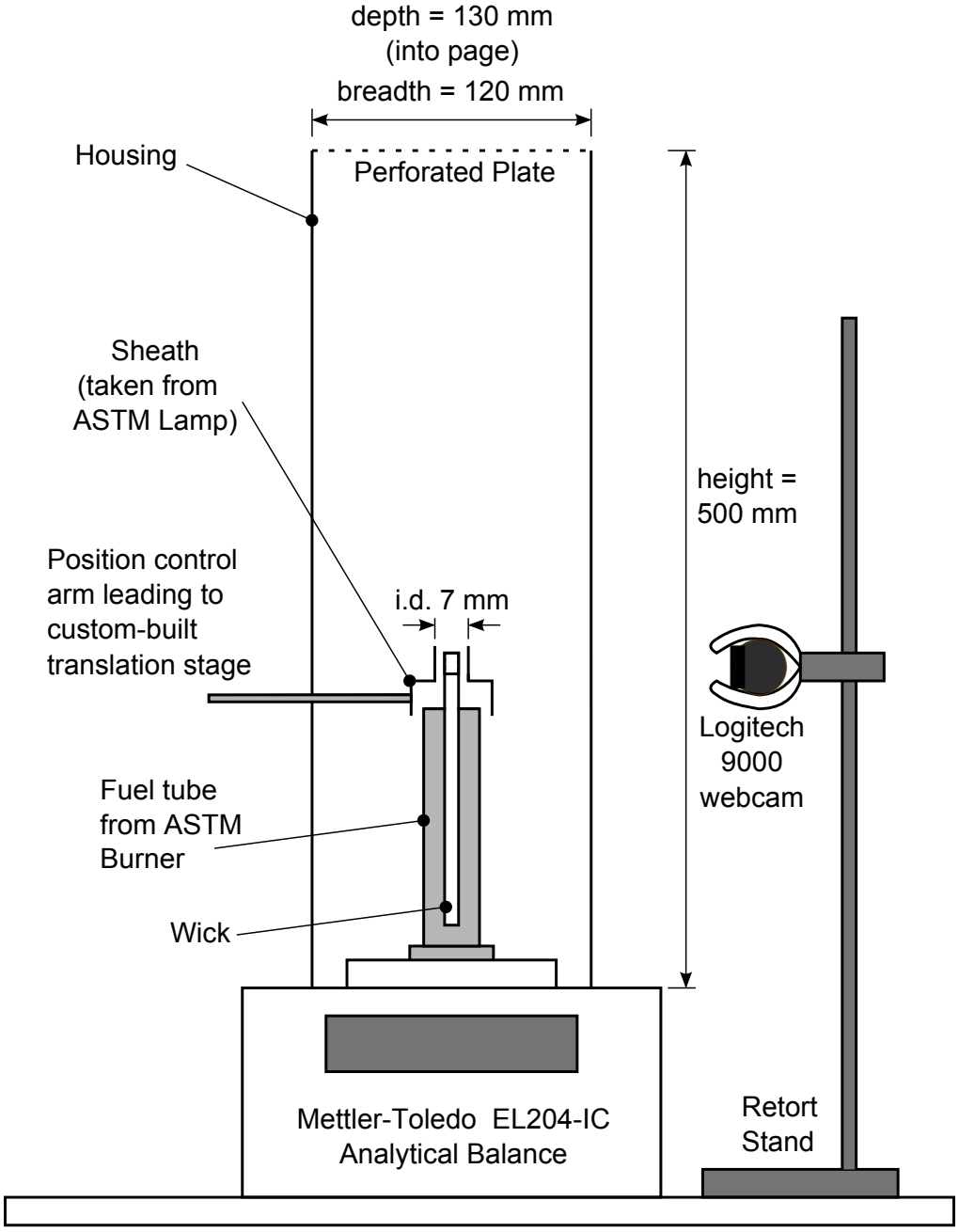

Figure 2: *Apparatus for determining flame height as a function of fuel uptake rate in a wick-fed burner.*

A MATLAB script was then used to automatically determine the position of the highest row to contain a white pixel for every frame of the footage; thus allowing calculation of the mean flame height as well as the statistical uncertainty in the value. This technique accounted for fluctuations in the flame height and established an objective measure of the tip position. The latter is particularly difficult to do by eye, because once the flame is above its smoke point the upper boundary of the flame ceases to be well-defined.

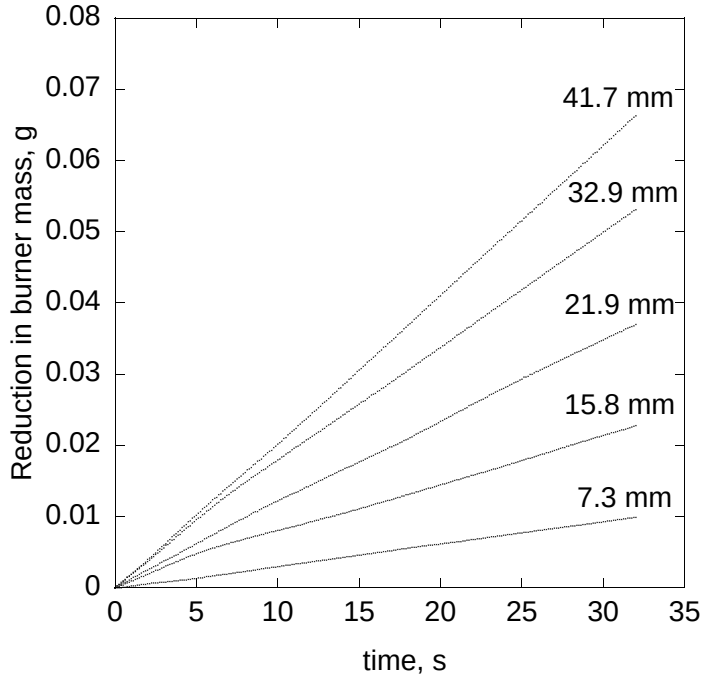

Figure 3: *Mass of fuel consumed vs time for a range of flame heights.*

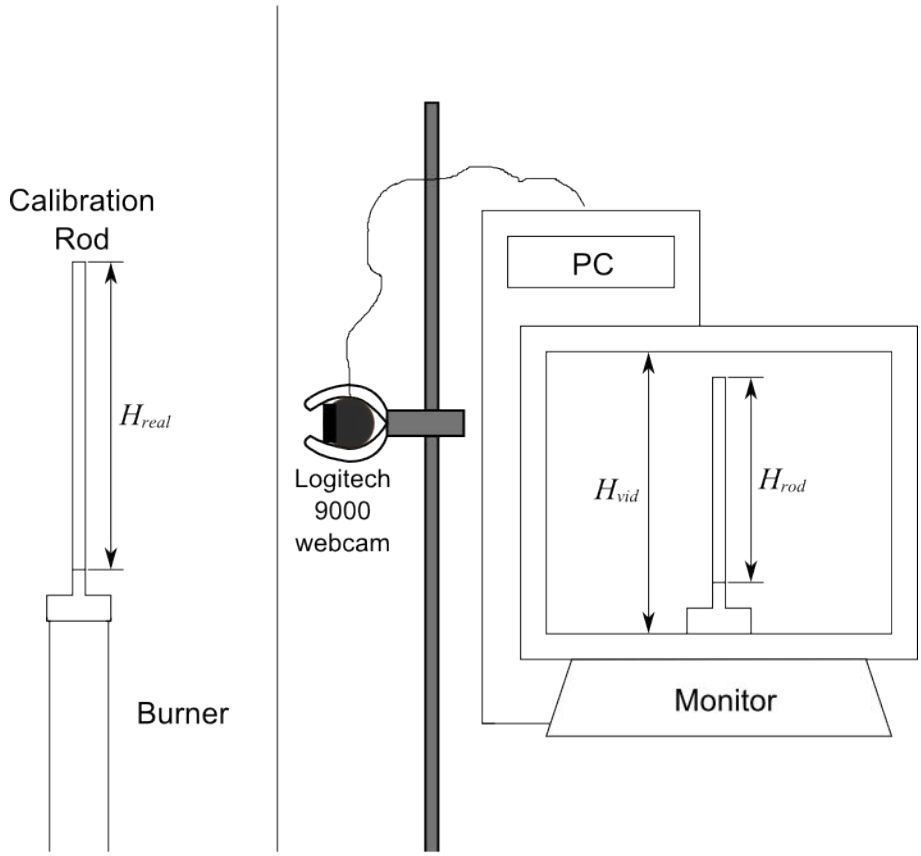

Figure 4: *Calibration of the Webcam*

3.2 Testing the New Methodology

The findings from the experiments described in section 3.1 indicated that there was potential to improve the reproducibility of the smoke point test by making certain alterations to the equipment and procedure used. In order to determine whether or not the current smoke point test should be adapted, three methodologies were compared:

1. The 'traditional' ASTM method, in which the flame wick sheath was adjusted until the flame morphology corresponded with point B in Figure 1a. The flame height was then measured using two rulers in front and behind in order to eliminate parallax error. Flame height was defined as the distance between the upper edge of the wick sheath and the tip of the flame.

2. The method of Olson et al. [13], which was identical to method 1, except that the fuel uptake rate was measured instead of the flame height.

3. A new method, in which the flame morphology was adjusted to resemble point A in Figure 1a, i.e. the point when the flame showed maximum sensitivity to adjustment and exhibited an intermittent smoke trail. The basis of this method is illustrated in **Figure** 7. If the smoke trail became permanent or completely disappeared after several minutes, the flame was adjusted until the trail became intermittent again. Once consistent instability was observed, the fuel uptake rate was measured.

For all fuels, each procedure was carried out 9 times by at least two different experimentalists, so that a true estimate of the experimental error could be obtained.

It was decided that the approach of simply weighing the burner before and after each trial in order to determine the fuel uptake rate was unsatisfactory, since it failed to take into account evaporation of the fuel either during the lighting of the flame or as the burner was being transferred to the balance. This problem was solved by continuous weighing of the burner followed by linear regression of the resulting values in order to determine the fuel uptake rate, as was done in section 2.4. For this approach to be viable, it was necessary to either use the setup shown in Figure 2, or redesign the burner so that its weight, including the flame adjustment mechanism, was less than the maximum allowed by the balance. The setup shown in Figure 2 was useful provided that the same fuel was used consistently, but required significant time and effort to adequately align the wick sheath so that it did not disrupt the balance readings every time the fuel was changed. The burner was therefore adapted by fitting a Delrin^{TM} thread to the outside of the burner tube and connecting this to the wick sheath via four brass struts, as depicted in **Figure** 5. Thus, the flame height could be adjusted by rotating the threaded fitting. Use of a Delrin^{TM} fitting was required, as a brass thread would have increased the weight beyond the maximum allowable by the balance.

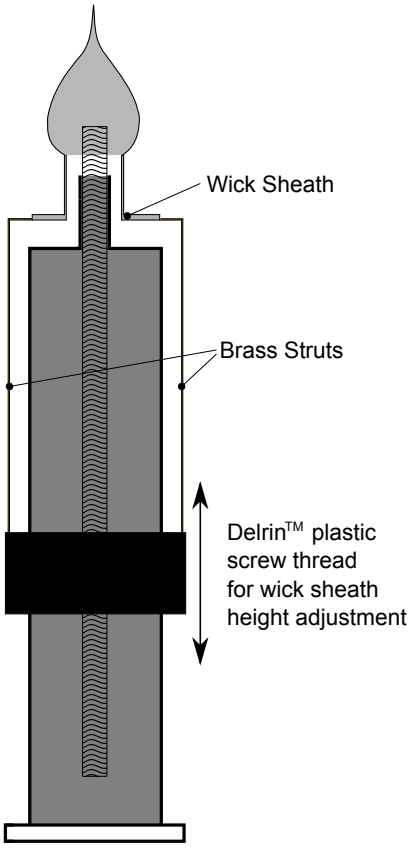

Figure 5: *The modified light-weight burner*

4 Results and Discussion

4.1 Relationship Between Flame Height and Fuel Uptake Rate

In order to confirm the findings of Olson et al. over a wide range of smoke points, a set of 10 toluene reference fuels was used, as outlined in table 1. The smoke points were determined using the ASTM D1322 criterion, applied to the setup in Figure 3. Percentages are given in terms of volume fraction of the component fuel.

Four of the flame height versus fuel uptake rate curves are displayed in **Figure** 6, together with the ASTM smoke point estimates as indicated by the thick horizontal line. There is some scatter in the data which falls outside the error bounds, and this is thought to be due mainly to interference between the sheath which is used to control the flame height and the cotton 'burr' at the top of the wick. The tendency of strongly sooting flames to fill the burner housing with large soot agglomerates is also a potential source of error. Furthermore, a trial had to be halted once the soot agglomerate concentration was too high to clearly view the flame, or if agglomerates began to fall back into the flame or wick assembly; which usually happened before the full range of the apparatus could be used. It should be noted that the flame height measurement was mildly dependent on

Table 1: *Toluene Reference fuel blends used in the flame height vs fuel uptake rate tests.*

Blend No.	Toluene (% vol.)	isooctane (% vol.)	n-heptane (% vol.)	Smoke Point (mm)	absolute error (±, 95% confidence)
1	100	0	0	7.3	1.2
2	66.7	16.67	16.67	10.8	1.3
3	50	50	0	12.3	1.4
4	50	0	50	13.7	1.4
5	33.3	33.3	33.3	16.5	3.1
6	16.67	66.7	16.67	21.7	2.6
7	16.67	16.67	66.7	25.7	7.4
8	0	100	0	38.1	7.3
9	0	50	50	53.2	7.0
10	0	0	100	72	18

ambient light levels, as these affected the results of the image processing; particularly for strongly sooting flames which showed a gradual fading of intensity at the tip. It is therefore recommended that any future measurements of this kind should be carried out in the dark.

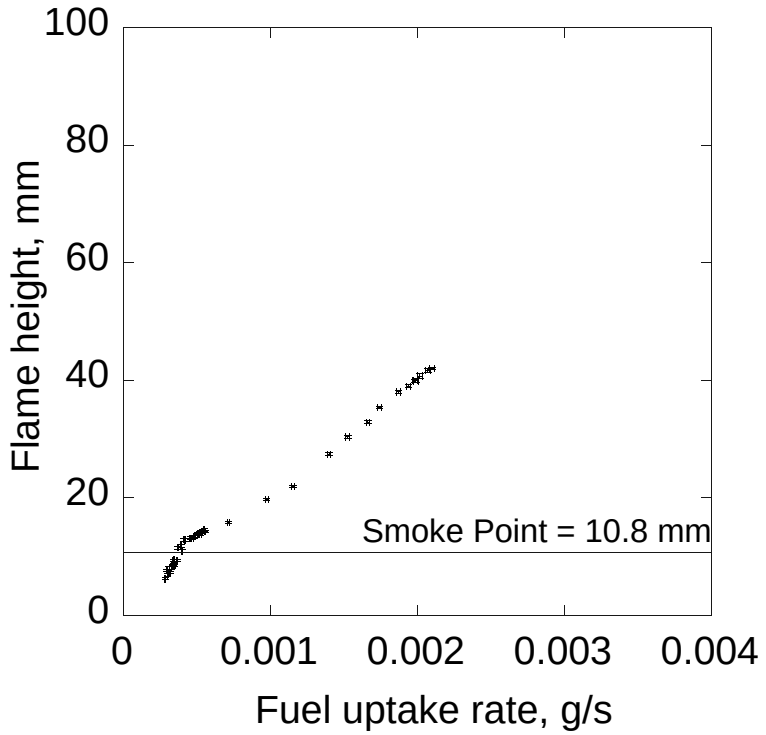

(a) *Blend 2 - 1:1:4 isooctane, n-heptane & toluene*

Figure 6: *Flame height vs fuel uptake rate curves for 10 toluene reference fuel blends.*

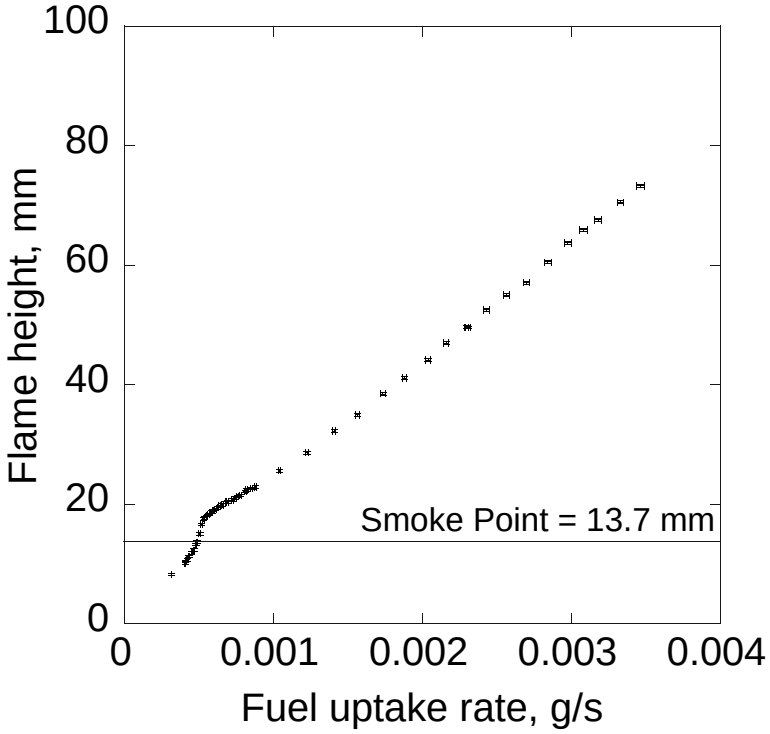

(b) *Blend 4 - 1:1 n-heptane & toluene*

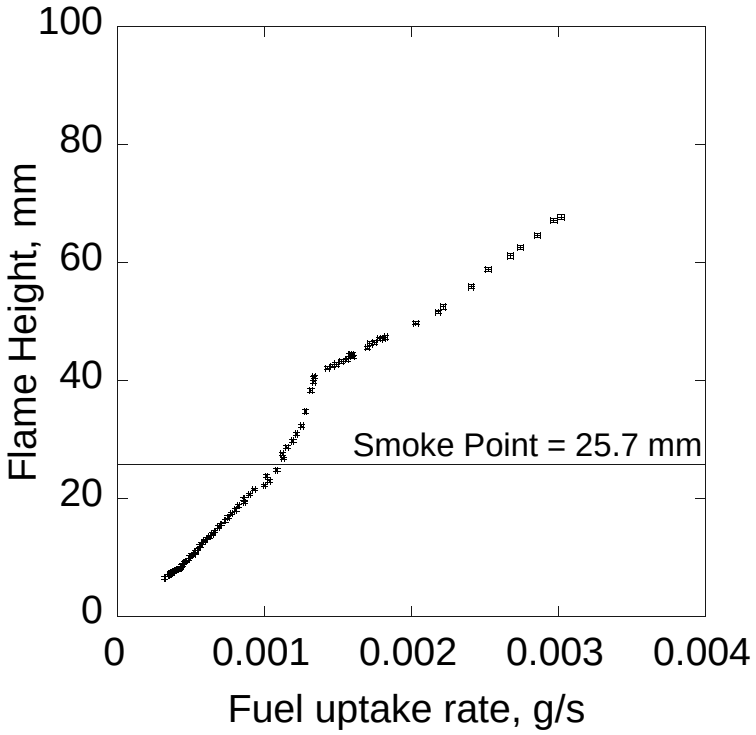

(c) *Blend 7 - 1:4:1 isooctane, n-heptane & toluene*

Figure 6: *Flame height vs fuel uptake rate curves for 10 toluene reference fuel blends*

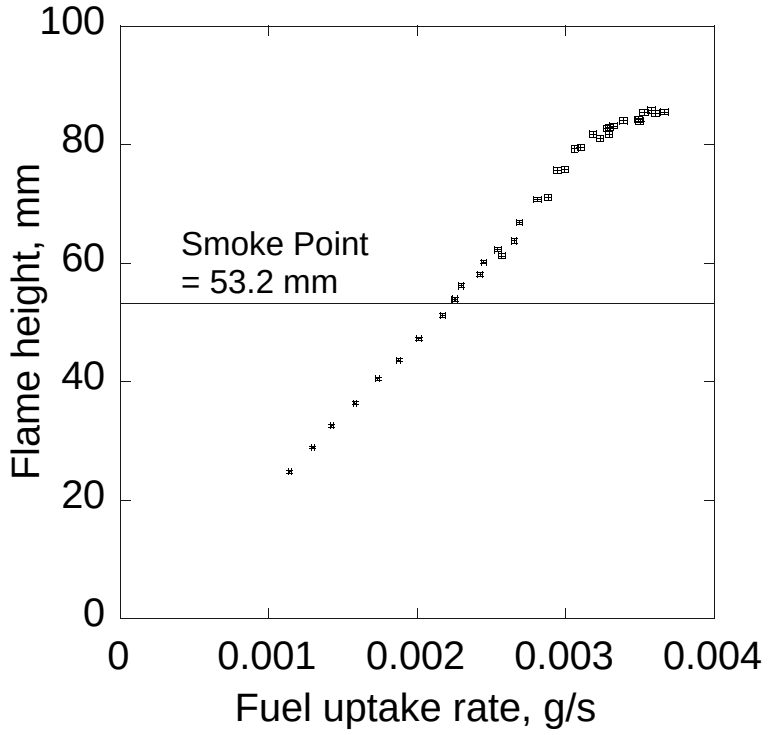

(d) *Blend 9 - 1:1 n-heptane & isooctane*

Figure 6: *Flame height vs fuel uptake rate curves for 10 toluene reference fuel blends*

Despite the limitations of the data, was observed that the distortion mentioned by Olson et al. was present in almost all cases, with the exception of pure n-heptane, where the the general trend suggests that any distortion would occur outside the range of the apparatus. For most of the blends, the data initially show a linear relationship between flame height and fuel uptake rate, before tending towards a vertical asymptote, then deviating sharply back to near-linearity. It is important to note that the smoke point seems to occur at or near the initial deviation from linearity, rather than the subsequent sharper deviation. This contradicts the findings of Olson et al. and implies that basing the TSI on the fuel uptake rate at the smoke point is unlikely to yield much improvement in reproduceability; because the smoke point occurs close to the linear region of the curve, the uptake rate and resulting TSI value will be subject to approximately the same level of human error as before.

By examining the video footage more closely, it was possible to identify certain flame morphologies with regions on the curve, as illustrated in Figure 7. In order to minimize the sensitivity to human error, it can be surmised that the best point to measure fuel uptake rate is when the flame height is most sensitive to wick adjustment just prior to the appearance of a soot trail, i.e the point where $\frac{dH}{d\dot{m}}$ is greatest.

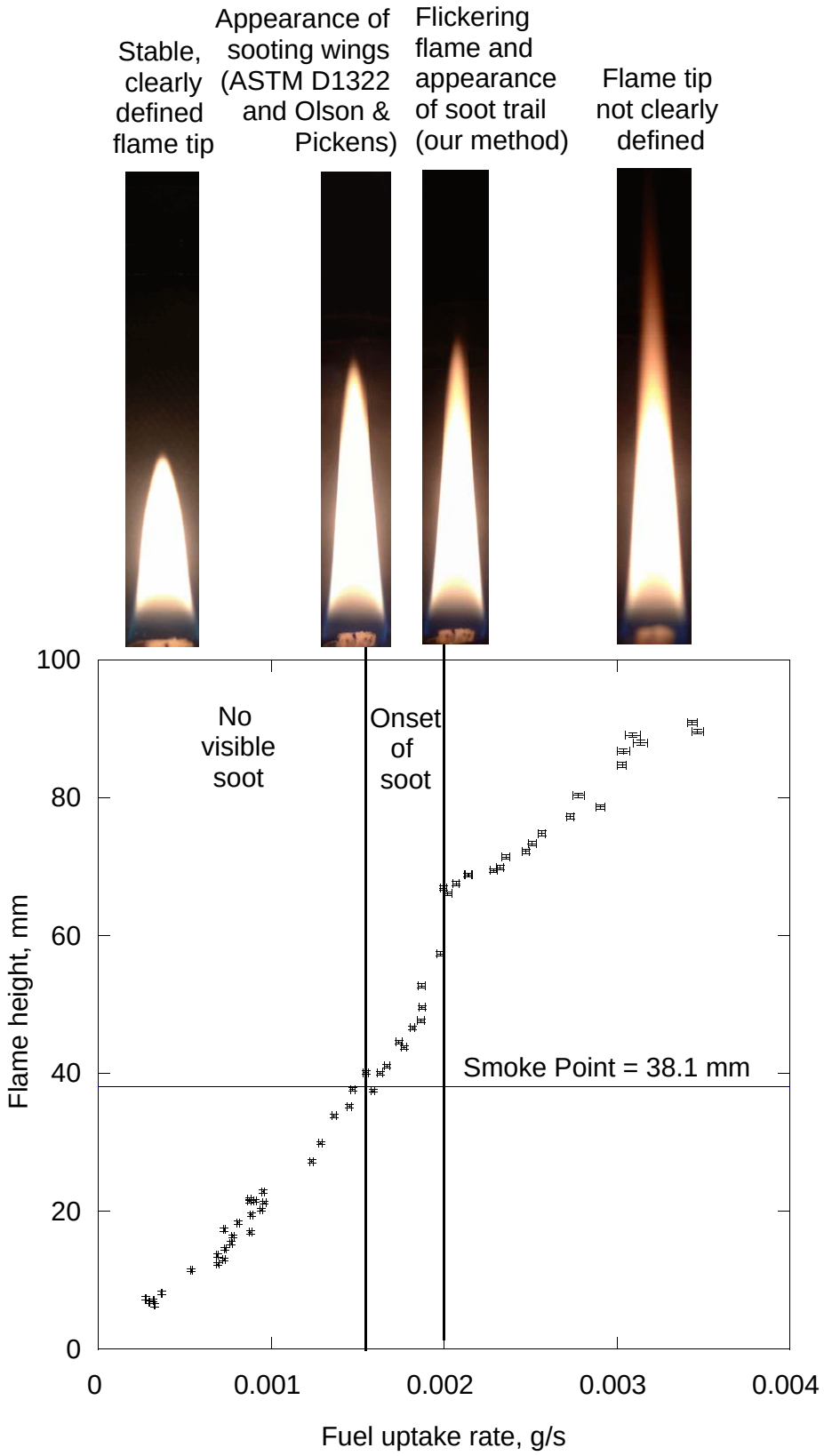

Figure 7: *Flame morphologies at important points on the flame height vs fuel uptake rate curve for blend 8.*

4.2 Comparing Methodologies

It was found that the percentage error in the raw values, i.e. smoke point and fuel uptake rate, were approximately halved by using the new method instead of the ASTM standard; however to gain a true estimate of the extent to which the new method is better, it is necessary to convert the raw measurements to TSI values, together with the associated error estimates.

Assuming that the TSI values for 1-methylnaphthalene and methylcyclohexane were 100 and 5 respectively, it was possible to calculate values for the coefficients a and b for each of the methods using equations (4) and (5). Using the standard methodology, error propagation equations were then used to derive equations (10) and (11) in order to gain an estimate of the overall errors, σ_a and σ_b, in the two coefficients:

$$\sigma_a = a\sqrt{\frac{\left(\frac{M_{W1}}{h_1^2}\sigma_{h1}\right)^2 + \left(\frac{M_{W2}}{h_2^2}\sigma_{h2}\right)^2}{\left(\left(\frac{M_{W1}}{h_1}\right) - \left(\frac{M_{W2}}{h_2}\right)\right)^2}} \tag{10}$$

$$\sigma_b = b\sqrt{\frac{\left(TSI_2\left(\frac{\sigma_{h1}M_{W1}}{h_1^2}\right)\right)^2 + \left(TSI_1\left(\frac{\sigma_{h2}M_{W2}}{h_2^2}\right)\right)^2}{\left(TSI_2\left(\frac{M_{W1}}{h_1}\right) - TSI_1\left(\frac{M_{W2}}{h_2}\right)\right)^2} + \frac{\left(\frac{M_{W1}}{h_1^2}\sigma_{h1}\right)^2 + \left(\frac{M_{W2}}{h_2^2}\sigma_{h2}\right)^2}{\left(\left(\frac{M_{W1}}{h_1}\right) - \left(\frac{M_{W2}}{h_2}\right)\right)^2}} \tag{11}$$

Where necessary, the fuel uptake rate and its error bounds could be substituted for the smoke point of the reference fuels, h_1 and h_2 and the associated errors, σ_{h1} and σ_{h2}. The results of the TSI calculations are summarized in table 2. Note that coefficient b is always dimensionless.

Table 2: *Coefficients in the TSI equation and associated errors for methods 1, 2 and 3*

Method	a	σ_a ($\pm$)	Units	b	σ_b ($\pm$)
Tratitional	4.06	0.75	mol g^{-1} mm^{-1}	-8.24	7.62
Olson & Pickens	1.06 $\times 10^{-4}$	7 $\times 10^{-6}$	mol s^{-1}	-2.67	1.29
New (this work)	1.18 $\times 10^{-4}$	4 $\times 10^{-6}$	mol s^{-1}	-1.12	0.25

The error in TSI is then given by equation (12)

$$\sigma_{TSI} = \sqrt{a^2\left(\frac{M_W}{h}\right)^2\left(\left(\frac{\sigma_a}{a}\right)^2 + \left(\frac{\sigma_h}{h}\right)^2\right) + \sigma_b^2} \tag{12}$$

The final TSI values and error bounds are shown in **Figure** 8 for blends and table 3 for pure components.Using the new method, blends of toluene and isocetane, ethanol, n-heptane and decanol were also investigated.

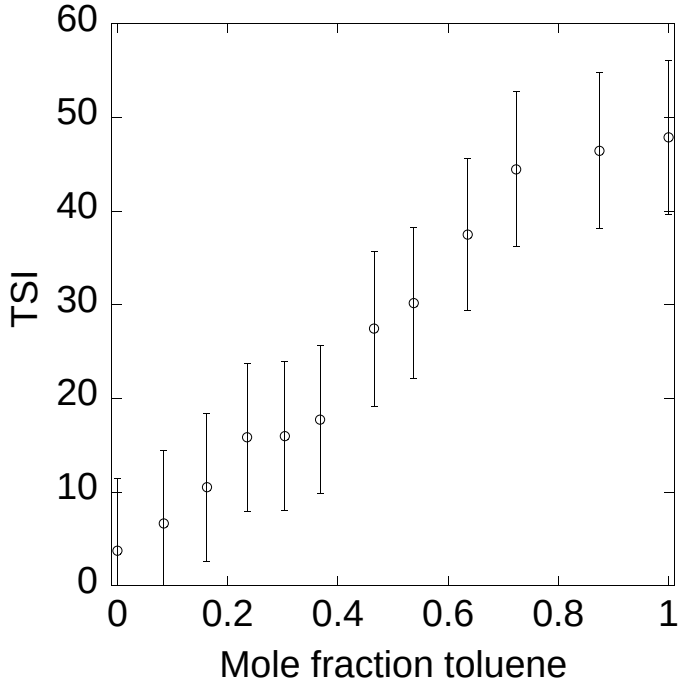

(a) *ASTM Method, isooctane-toluene blend*

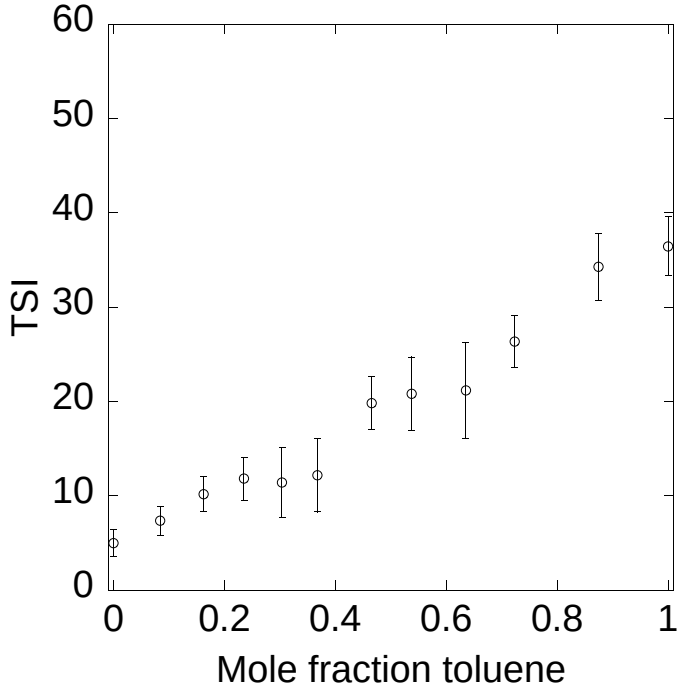

(b) *Method of Olson & Pickens, isooctane-toluene blend*

Figure 8: *TSIs, based on a variety of methods, for a variety of component fuels blended with toluene.*

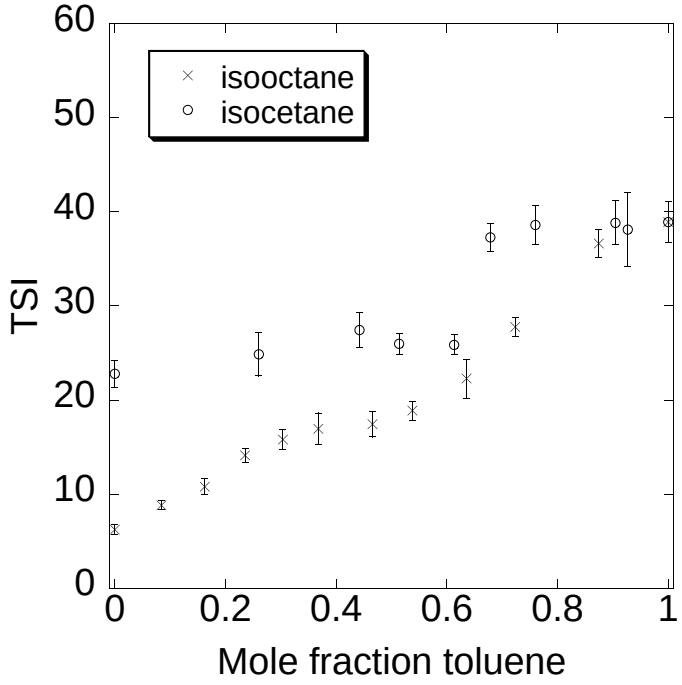

(c) *New Method (this work)*

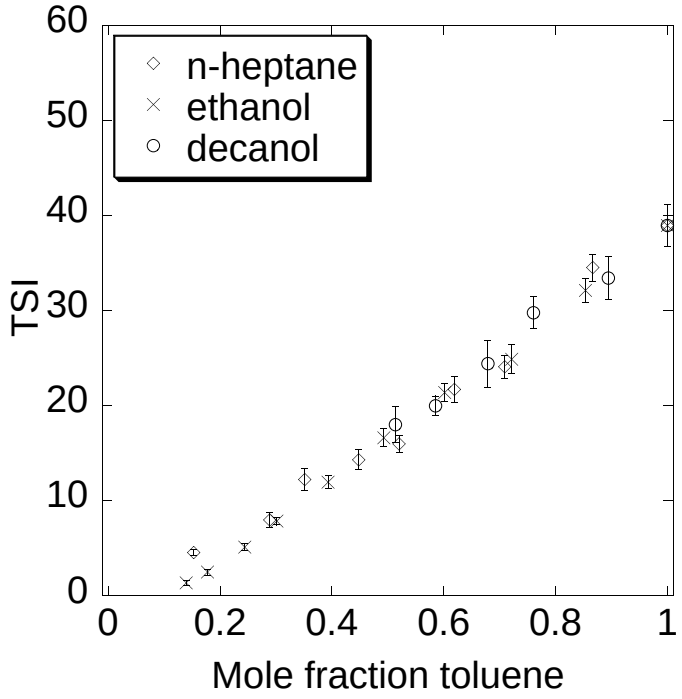

(d) *Other experimental data obtained using the new method described in this work.*

Figure 8: *TSIs, based on a variety of methods, for a variety of component fuels blended with toluene.*

Table 3: *TSI values and associated error bounds for the ASTM, Olson & Pickens (O & P) and New methods.*

Fuel	TSI, ASTM			TSI, O & P			TSI, New		
		Error			Error			Error	
		±	%		±	%		±	%
1-Methylnaphthalene	100.0	9.2	**9.18**	100.0	9.4	**9.4**	100.0	4.7	**4.7**
50% n-heptane, 50% tol.	33.0	8.1	**24.6**	18.8	3.2	**20.0**	21.0	2.0	**11.3**
66% n-heptane, 33% tol.	14.9	1.2	**8.4**	684	82	**11.9**	742	42	**5.7**
75% n-heptane, 25% tol.	16.2	7.9	**48.7**	11.3	3.7	**32.6**	15.9	1.6	**10.0**
Phenylcyclohexane	108.9	11.2	**10.3**	66.4	6.4	**9.7**	69.2	3.2	**4.6**
methylcyclohexane	5.0	7.8	**156**	5.0	1.8	**36.2**	5.0	0.4	**7.2**

In order to compare the results from each method, the isooctane-toluene data are plotted together on **Figure** 8, together with the loci of the error estimates for each data set:

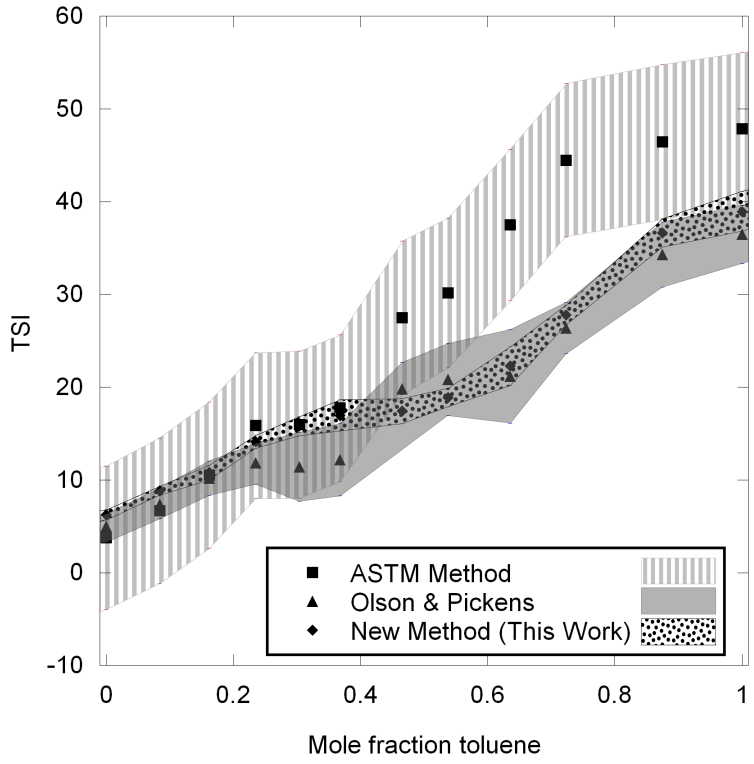

Figure 9: *Comparison of results for blends of iso-octane and toluene for each method, showing the loci of the 95% confidence intervals.*

It can be seen from table 3 and Figure 8 that the errors in the TSI values for the ASTM method were generally much higher than the value of 15% quoted in the literature [9],

to the extent that the lower TSI values are essentially meaningless. Presumably this is because the error in the calibration procedure itself is rarely taken into account; which might explain the wide variation in the literature TSI values. Figure 8 is also of interest because is shows that the two methods based on fuel uptake rate give consistent results, despite the difference in the way the measurement is taken. In contrast, the results from the ASTM method appeared to be inconsistent with both of the other methods. These facts suggest that there is either a significant measurement artifact for one or both of the methods, or that the relationship between $\dot{m}$ and h is non-linear and that the theory of Burke and Schumann [2] is an oversimplification for the case of interest.

Figure ?? suggests that there might also be some non-linearity in the TSI blending. Non-linear blending was not as strongly supported by previous literature results [10] for isooctane-toluene blends, and was therefore thought to be an artifact of the measurement which affects the new method more than the ASTM method.

The most likely explanation for this measurement artifact is illustrated in **Figure** 10. In some cases vapor condensate was observed to leave the base of the wick sheath in the form of a fine mist, particularly for blends of molar composition 20-40% aromatic. presenting compelling evidence that vapor downflow is the cause of the distortion in the TSI blending curve. Such behavior is typically characterized by a concave flame front, which is caused by the base of the flame expanding to compensate for the lack of air flowing up the sheath. Vapor downflow could significantly affect the results, as the fuel uptake rate will be artificially inflated relative to the height of the flame, thus reducing the TSI value. A return to the ASTM method would only partially address the problem, as the component fuels have differing vapor pressures and are almost certain to fractionate between the fuel being burnt and the fuel escaping from the base of the wick sheath. Since fuels of high sooting propensity tend to have lower vapor pressures, disproportionate splitting is likely to inflate the smoke point as well. Most variants of the smoke point test are therefore likely to give artificially reduced TSI values for at least some fuel blends.

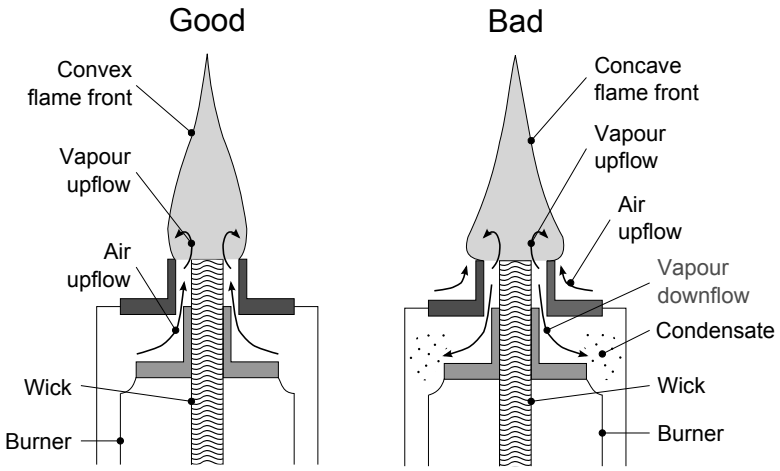

Figure 10: *Escape of vapor condensate from the base of the wick sheath.*

The standard lamp used by Mensch et al. [10] would have had a narrower annular gap than the lamp used in this work, and while this might explain the greater linearity of the blending in their results, it is clear that some non-linearity remains. It is difficult to eliminate vapor downflow by closing the annular gap altogether, as experience has shown that surface tension effects cause the fuel to overflow from the wick; resulting in a pool fire which is both hazardous and of no value for determining the TSI.

5 Conclusions

A new method for determining Threshold sooting indices is been proposed in which the fuel uptake rate is measured at the point when the flame height exhibits maximum sensitivity to adjustment and an intermittent soot trail is observed, characterized by flickering of the flame. The method has been shown to yield results which are typically subject to less than half the statistical uncertainty of other previously reported methods using similar apparatus; however it was also found that under some conditions unburnt vapor can escape, resulting in distorted TSI measurements. This distortion is a flaw inherent to smoke point lamp techniques when used with certain fuel blends, which is merely amplified by the new method. The new method nevertheless delivers improved results in the majority of cases, particularly for aromatics, and the fuel blends for which it is unsuited are easily identifiable from the flame morphology.

6 Acknowledgements

We gratefully acknowledge the contributions of Mr Rui Hui and Mr Chin Kiat Tan, who assisted with the experimental work described in this paper as part of their respective degree courses; the invaluable feedback from our colleagues Dr Andrew Smallbone, Dr Sebastian Mosbach and Dr Jethro Ackroyd; the technical support from Mr Lee Pratt and Mr Jon Cowper; and the provision of facilities by the Department of Chemical Engineering & Biotechnology, University of Cambridge.

7 Appendices

7.1 Smoke Point Results

Table 4: *Smoke points and critical fuel uptake rates for the ASTM, Olson & Pickens (O & P) and New methods.*

Fuel	ASTM, smoke point (mm)			O & P, Fuel uptake rate (μg/s)			New, Fuel uptake rate (μg/s)		
		Error			Error			Error	
		$\pm$	%		$\pm$	%		$\pm$	%
1-Methylnaphthalene	5.3	0.9	**16.1**	147	9	**6.1**	166	5	**3.2**
Phenylcyclohexane	5.6	1.8	**32.8**	246	15	**6.2**	269	8	**3.0**
toluene	5.6	1.7	**30.0**	308	47	**15.2**	333	27	**8.1**
50% n-heptane, 50% tol.	11.1	0.8	**7.4**	471	60	**12.8**	494	25	**5.1**
50% isooctane, 50% tol.	8.9	0.9	**10.3**	448	87	**19.4**	484	69	**14.3**
60% isooctane, 40% tol.	11.2	1.2	**10.5**	477	68	**14.2**	525	52	**10.0**
66% n-heptane, 33% tol.	14.9	1.2	**8.4**	684	82	**11.9**	742	42	**5.7**
66% isooctane, 33% tol.	11.9	2.3	**19.6**	493	44	**9.0**	552	57	**10.4**
75% n-heptane, 25% tol.	17.5	1.9	**11.1**	769	71	**9.2**	865	67	**7.8**
75% isooctane, 25% tol.	16.7	1.6	**9.6**	762	182	**23.8**	696	60	**8.6**
80% isooctane, 20% tol.	18.1	2.2	**12.4**	814	194	**23.9**	753	37	**4.9**
85% isooctane, 15% tol.	18.4	1.4	**7.7**	801	90	**11.2**	847	26	**3.1**
90% isooctane, 10% tol.	24.0	3.5	**14.5**	917	71	**7.8**	1098	61	**5.5**
95% isooctane, 5% tol.	30.7	4.3	**14.0**	1191	65	**5.5**	1335	36	**2.7**
iso-octane	38.7	1.4	**3.7**	1582	74	**4.7**	1832	106	**5.8**
methylcyclohexane	30.1	4.0	**13.4**	1360	207	**15.3**	1894	52	**2.7**

Table 5: *TSI values and associated error bounds for the ASTM, Olson & Pickens (O & P) and New methods.*

Fuel	TSI, ASTM			TSI, O & P			TSI, new		
		Error			Error			Error	
		$\pm$	%		$\pm$	%		$\pm$	%
toluene	48.8	9.3	**19.1**	24.3	4.7	**19.2**	26.6	2.5	**9.2**
50% isooctane, 50% tol.	23.4	7.9	**34.0**	16.8	4.66	**24.4**	19.5	3.3	**15.5**
60% isooctane, 40% tol.	22.2	8.0	**35.9**	16.0	3.1	**18.4**	17.7	1.3	**6.6**
66% isooctane, 33% tol.	16.4	7.9	**48.1**	11.3	2.3	**20.3**	13.2	1.0	**7.4**
75% isooctane, 25% toluene	13.2	7.9	**59.7**	10.1	1.9	**19.2**	11.5	1.1	**9.5**
80% isooctane, 20% tol.	14.8	7.9	**53.5**	10.7	3.6	**33.2**	15.0	1.0	**6.6**
85% isooctane, 15% tol.	15.0	7.9	**52.6**	11.3	2.2	**19.7**	13.6	0.7	**5.3**
90% isooctane, 10% tol.	10.0	7.9	**78.5**	9.8	1.8	**18.4**	10.5	0.8	**7.6**
95% isooctane, 5% tol.	6.5	7.8	**121**	7.2	1.5	**21.4**	8.7	0.5	**5.6**
iso-octane	3.8	7.7	**206**	5.0	1.4	**28.6**	6.2	0.6	**8.8**

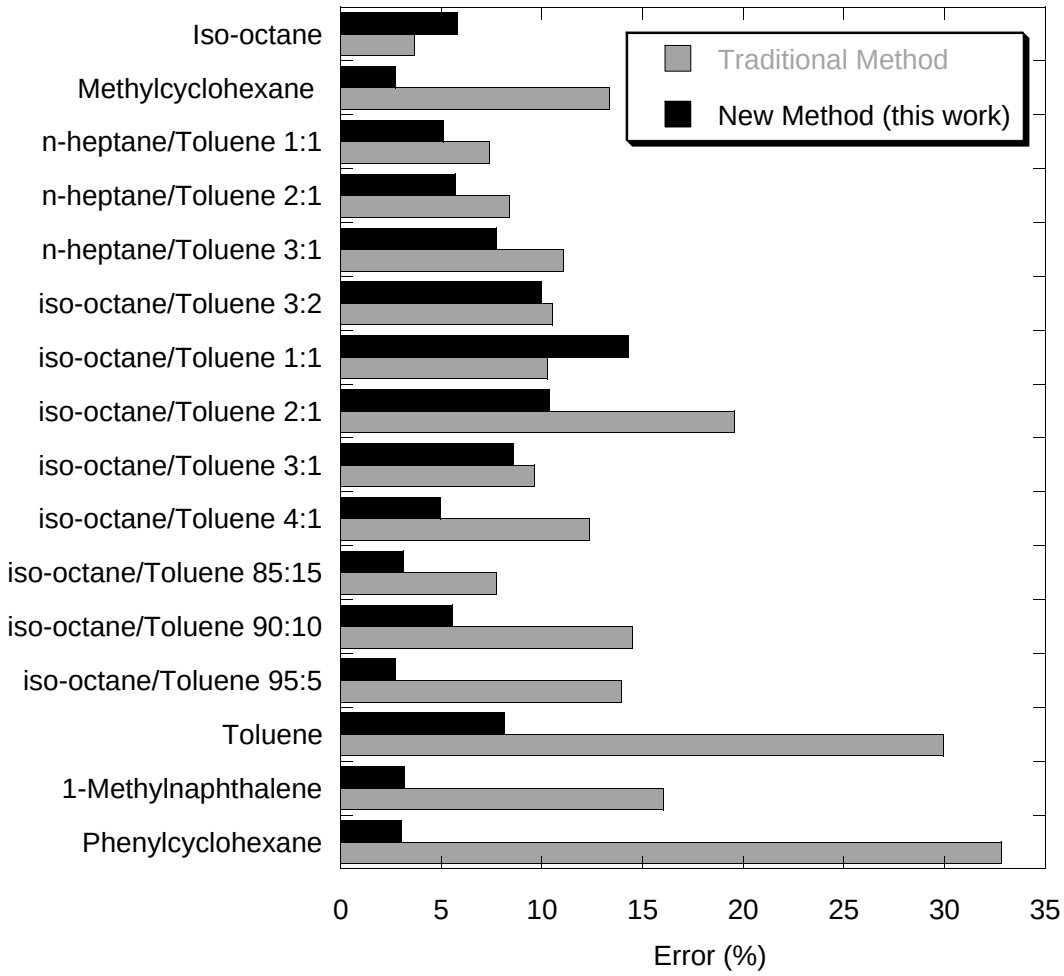

Figure 11: *Comparison of experimental errors in raw results from the ASTM and new methods*

7.2 Error Analysis

In order to estimate how errors in smoke point translate through to errors in TSI, Taylor expansions of generic functions are used to derive the simple rules shown in Table 6:

Table 6: *Basic rules of error propagation for a function, f, where σf is the uncertainty associated with the value of the function f.*

Function	Standard Error	
1	$f = A \pm B$	$\sigma_f = \sqrt{\sigma_A^2 + \sigma_B^2}$
2	$f = xA^{\pm y}$	$\sigma_f = yf\frac{\sigma_A}{A}$
3	$f = AB, f = \frac{A}{B}$	$\sigma_f = f\sqrt{(\frac{\sigma_A}{A})^2 + (\frac{\sigma_B}{B})^2}$

The reference fuels, namely 1-methylnaphthalene and methylcyclohexane, are used to calibrate the apparatus (i.e. to find a and b). Referring to these fuels using subscripts 1 and 2 respectively, their TSI values are given by equations 15 and 16:

$$TSI_1 = a\left(\frac{M_W}{h_1}\right) + b \qquad (13) \qquad\qquad TSI_1 = a\left(\frac{M_W}{h_2}\right) + b \qquad (14)$$

where M_W and h are the molecular weights and smoke points respectively of fuels 1 and 2. Hence by simultaneous solution:

$$a = \frac{TSI_1 - TSI_2}{\left(\frac{M_W}{h_1}\right) - \left(\frac{M_W}{h_2}\right)} \qquad (15) \qquad\qquad b = \frac{TSI_2\left(\frac{M_W}{h_1}\right) - TSI_1\left(\frac{M_W}{h_2}\right)}{\left(\frac{M_W}{h_1}\right) - \left(\frac{M_W}{h_2}\right)} \qquad (16)$$

Using a special case of rule 3 in table 6, the 95% confidence interval in a function of the form $f = k/A$ is given by:

$$\sigma_f = k\sigma_A/A^2 \qquad (17)$$

Applying rules 1 and 3 from table 6 as well as Equation 17, yields Equations 18 and 19:

$$\sigma_a = a\sqrt{\frac{\left(\frac{M_{W1}}{h_1^2}\sigma_{h1}\right)^2 + \left(\frac{M_{W2}}{h_2^2}\sigma_{h2}\right)^2}{\left(\left(\frac{M_{W1}}{h_1}\right) - \left(\frac{M_{W2}}{h_2}\right)\right)^2}} \qquad (18)$$

$$\sigma_b = b\sqrt{\frac{\left(TSI_2\left(\frac{\sigma_{h1}M_{W1}}{h_1^2}\right)\right)^2 + \left(TSI_1\left(\frac{\sigma_{h2}M_{W2}}{h_2^2}\right)\right)^2}{\left(TSI_2\left(\frac{M_{W1}}{h_1}\right) - TSI_1\left(\frac{M_{W2}}{h_2}\right)\right)^2} + \frac{\left(\frac{M_{W1}}{h_1^2}\sigma_{h1}\right)^2 + \left(\frac{M_{W2}}{h_2^2}\sigma_{h2}\right)^2}{\left(\left(\frac{M_{W1}}{h_1}\right) - \left(\frac{M_{W2}}{h_2}\right)\right)^2}} \qquad (19)$$

Note that the reference TSIs are defined values and hence have no associated experimental error.

Nomenclature

Lower-case Roman

M_W	Molecular weight of fuel,	g mol^{-1}
h	Smoke point,	mm
a, b	Apparatus-dependent constants,	variable units
C, D	constants in the YSI equation	-

N_P	Length of the video image of the flame	pixels
H_{real}	Actual flame height,	mm
H_{rod}	Height of the video image of the calibration rod,	mm
H_{vid}	Overall height of the video image,	mm
x_f	Mole fraction of component fuel	-
$f_{v;max}$	Maximum soot volume fraction	-

Lower-case Greek

θ	equivalence ratio, dimensionless
σ	error, various dimensions

Subscripts

1	Value for the reference fuel with the higher TSI
2	Value for the reference fuel with the lower TSI
h	constants determined based on smoke point measurements
e	constants determined based on critical equivalence ratio
V	constants determined based on volumetric flow rate of fuel
pure	refers to pure fuel
blend	refers to blended fuel

Abbreviations

TSI	Threshold Sooting Index
YSI	Yield Sooting Index

References

[1] W. S. Blazowski. Dependence of soot production on fuel structure in back-mixed combustion. *Combustion Science and Technology*, 21(3-4):87–96, 1980. doi:10.1080/00102208008946922.

[2] S. P. Burke and T. E. W. Schumann. Diffusion flames. *Industrial and Engineering Chemistry*, 20(10):1–7, 1928. doi:10.1021/ie50226a005.

[3] H. F. Calcote and D. M. Manos. Effect of molecular structure on incipient soot formation. *Combustion and Flame*, 49(1-3):289–304, 1983. doi:10.1016/0010-2180(83)90172-4.

[4] S. P. Crossley, W. E. Alvarez, and D. E. Resasco. Novel micropyrolyis index (mpi) to estimate the sooting tendency of fuels. *Energy and Fuels*, 22(4):2455–2464, 2008.

[5] R. Gill and D. Olson. Estimation of soot thresholds for fuel mixtures. *Combustion Science and Technology*, 40(5):307–315, 1984.

[6] I. Glassman and P. Yaccarino. The temperature effect in sooting diffusion flames. *Eighteenth Symposium (International) on Combustion*, 1981.

[7] J. L. Jezl. Report no. d1016. Technical report, Sun Oil Co., Research and Development, 1950.

[8] C. McEnally and L. de Pfefferle. Sooting tendencies of oxygenated hydrocarbons in laboratory-scale flames. *Environmental Science and Technology*, 45(6):24982503, 2011.

[9] C. S. McEnally and L. D. Pfefferle. Improved sooting tendency measurements for aromatic hydrocarbons and their implications for naphthalene formation pathways. *Combustion and Flame*, 148(4):210–222, 2007.

[10] A. Mensch, R. J. Santoro, T. A. Litzinger, and S. Y. Lee. Sooting characteristics of surrogates for jet fuels. *Combustion and Flame*, 157:1097–1105, 2010.

[11] S. Minchin. Luminous stationary flames: The quantitative relationship between flame dimension at the sooting point and chemical composition. *Jour. Inst. Petroleum Technologists*, 17:102, 1931.

[12] S. Mosbach, M. Celnik, A. Raj, M. Kraft, H. Zhang, S. Kubo, and K. Kim. Towards a detailed soot model for internal combustion engines. *Combustion and Flame*, 156: 1156–1165, 2009.

[13] D. Olson, J. Pickens, and R. Gill. The effects of molecular structure on soot formation ii. diffusion flames. *Combustion and Flame*, 62(1):43–60, 1985.

[14] C. A. Pope and D. W. Dockery. Health effects of fine particulate air pollution: Lines that connect. *Journal of the Air and Waste Management Association*, 56:709742, 2006.

[15] A. Raj, P. Man, T. Totton, M. Sander, R. Shirley, and M. Kraft. New polycyclic aromatic hydrocarbon (pah) surface processes to improve the model prediction of the composition of combustion-generated pahs and soot. *Carbon*, 48:319–332, 2010.

[16] A. Raj, M. Sander, V. Janardhanan, and M. Kraft. A study on the coagulation of polycyclic aromatic hydrocarbon clusters to determine their collision efficiency. *Combustion and Flame*, 157:523–534, 2010.

[17] F. W. Rakowsky and R. A. Hunt. Variables in lamp design that affect smoke point. *Analytical Chemistry*, 28(10):1583–1586, 1956. doi:10.1021/ac60118a024.

[18] R. Schalla and G. McDonald. Variation in smoking tendency among hydrocarbons of low molecular weight. *Industrial and Chemical Chemistry*, 45(7):1497–1500, 1953.

[19] A. Seaton, D. Godden, W. MacNee, and K. Donaldson. Particulate air pollution and acute health effects. *The Lancet*, 345(8943):176–178, 1995.

[20] J. C. Street and A. Thomas. Carbon formation in premixed flames. *Fuel*, 34(4): 4–36, 1955.

[21] T. Totton, D. Chakrabarti, A. Misquitta, M. Sander, D. Wales, and M. Kraft. Modelling the internal structure of nascent soot particles. *Combustion and Flame*, 157: 909–914, 2010.

[22] Y. Yang, A. L. Boehman, and R. J. Santoro. A study of jet fuel sooting tendency using the threshold sooting index (tsi) model. *Combustion and Flame*, 149(1-2): 191–205, 1985.

Citation index